ANALYTICAL SCIENCE & TECHNOLOGY
(Journal of the Korean Society of Analytical Sciences)
Vol. 8, No. 4, 1995
Printed in the Republic of Korea

Applications of Scanning Electrochemical Microscopy

Allen J. Bard and Fu-Ren F. Fan

Department of Chemistry and Biochemistry, The University of Texas at Austin, Austin, Texas 78712 U.S.A.

Abstract: The application of scanning electrochemical microscopy to the imaging of surfaces in water and air and to the study of the electrochemistry of single molecules is discussed.

Keywords: Scanning Electrochemical Microscopy (SECM), Single-Molecule Detection (SMD), Redox Reaction.

Introduction

Scanning electrochemical microscopy (SECM) involves the use of a small electrode moved very near a surface in an electrochemical cell arrangement to obtain information about the surface topography and reactivity and about reactions that occur in the solution space between the tip and sample. Because this technique has been the subject of several recent detailed reviews [2-4], only a brief discussion of the general principles, theory, and instrumentation will be given here, and most of the discussion will be devoted to the application of SECM to the imaging of surfaces in solution and in air and its ability to study the electrochemistry of single molecules.

SECM Principles

The SECM is based on the changes in the faradaic current that flows during a redox process at a tip as it moves above a substrate that is immersed in a solution containing an appropriate species in the oxidized (Ox) or reduced (Red) state. In addition to the tip electrode, auxiliary and reference electrodes are immersed in the solution to form an electrochemical cell, and the potential of the tip is controlled by a potentiostat [5]. For example, if the solution contains the species Ox (e.g., Fe^{3+}) and the tip potential is adjusted with respect to the reference electrode to reduce Ox at a mass-transfer-controlled rate, the reaction Ox + $ne \rightarrow$ Red occurs. If the ultramicroelectrode tip is far from any substrate, the steady-state current that flows, $i_{T,\infty}$, is given by equation 1 [6]

$$i_{T,\infty} = 4nFDca \qquad (1)$$

where F is the Faraday, c is the concentration of Ox, D is its diffusion coefficient, and a is the radius of the tip. This current represents the flux of Ox to the electrode through the essentially hemispherical diffusion layer around the tip. However, when the tip is close to the substrate, i.e., within a few tip

radii, the current is perturbed by the presence of the substrate. If the reverse reaction Red → Ox + *ne* cannot occur on the substrate, e.g., if the substrate is an electrical insulator that does not react with Red, the current will be smaller than $i_{T,\infty}$, because the substrate simply blocks the diffusion of Ox to the tip. In SECM parlance, this effect is termed negative feedback. For a conductive substrate, the oxidation of Red to Ox can occur. This provides an additional source of Ox for the tip, and the current observed is greater than $i_{T,\infty}$. Thus when the reverse reaction can occur at the substrate, positive feedback is observed. These principles are illustrated in Figure 1. In general, in SECM the relative magnitude of the current (i_T) compared to $i_{T,\infty}$ is a measure of the distance between the tip and substrate, d, and depends upon the nature of the substrate.

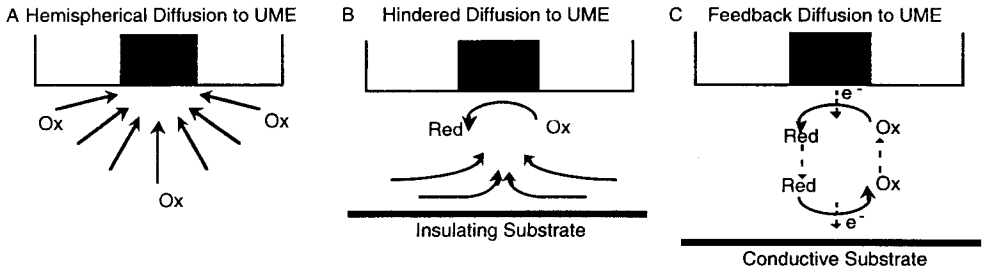

Fig. 1. Basic principles of SECM. (A) With the ultramicroelectrode (UME) tip far from substrate, diffusion leads to a steady-state current $i_{T,\infty}$. (B) UME near an insulating substrate. Hindered diffusion leads to $i_T < i_{T,\infty}$. (C) UME near a conductive substrate. Positive feedback leads to $i_T > i_{T,\infty}$. (Reprinted from A. J. Bard, F.-R. F. Fan, D. T. Pierce, P. R. Unwin, D. O. Wipf and F. Zhou, *Science*, **254**, *68* (1991). Copyright 1991 American Association for the Advancement of Science.]

An advantage of SECM compared to other scanning probe microscopies, e.g., scanning tunneling microscopy (STM), is that the theoretical behavior is readily accessible through typical electrochemical diffusion-kinetic treatments [3,7-12]. Curves can be cast in the dimensionless form of $i_T/i_{T,\infty}$ versus d/a, which are independent of solution concentration and diffusion coefficient. Curves showing the predicted behavior for an unreactive insulator (i.e., a material where the rate constant, k_f, of the Red → Ox reaction is 0) and for a conductive substrate (where $k_f \rightarrow \infty$) are shown in Figure 2. Thus by measuring the $i_T/i_{T,\infty}$ ratio, one can immediately estimate the tip-substrate distance d, if the tip radius a is known. When the rate constant of the Red → Ox reaction is of an intermediate value, i.e., $0 < k_f < \infty$, a family of curves is obtained that spans the behavior between the two limits illustrated in Figure 2 [10,13]. The dependence of $i_T/i_{T,\infty}$ on k_f allows one to carry out reaction-rate imaging of surfaces, as discussed below.

The apparatus used for SECM [1,4] basically combines electrochemical and STM instrumentation. Thus a potentiostat (or a bipotentiostat, if the substrate potential is controlled) is used to adjust the tip potential with respect to the reference electrode [5]. The tip is moved toward and away from the substrate (the z direction) and across the surface (x and y directions) by means of piezoelectric scanners. Tip potential and position are adjusted via a digital computer and the associated A/D and D/A cards. This arrangement allows one to obtain approach curves of $i_T/i_{T,\infty}$ versus d/a, and surface scans showing i_T at a given d as a function of x,y position. SECM scans with tip position modulation and constant current operation are also possible [14,15].

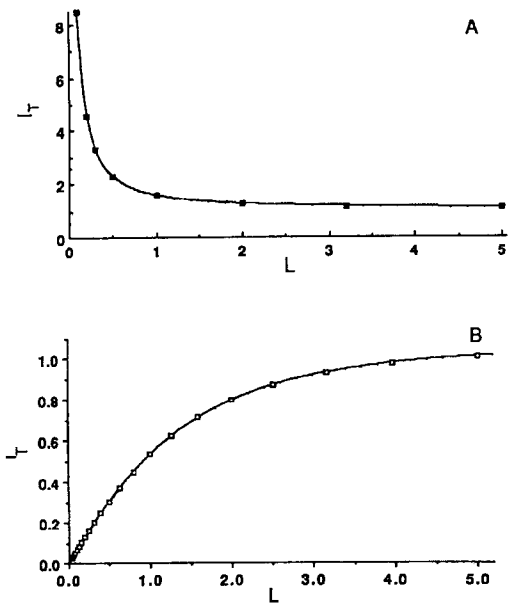

Fig. 2. Diffusion-controlled steady-state normalized tip current ($I_T = i_T/i_{T,\infty}$) as a function of dimensionless tip-substrate separation ($L = d/a$). (A) Substrate is a conductor where the reverse reaction is diffusion-controlled. (B) Substrate is an unreactive insulator. [Reprinted from A. J. Bard, F.-R. F. Fan and M. V. Mirkin, in "Electroanalytical Chemistry", Vol. 18, A. J. Bard, Ed., Marcel Dekker, New York, 1994, p 243. Copyright 1994 Marcel Dekker.)

Imaging

Many different types of surfaces have been imaged by SECM, including electrodes, minerals, semiconductors, membranes and biological specimens [2-4]. Most of these imaging studies have been carried out in the constant height mode, where the tip is rastered across the substrate at a constant reference plane above the sample surface and variations in the tip current are recorded. These are then used to produce topographic plots or gray-scale images of the sample surfaces. The resolution obtainable in SECM is governed by the size of the tip and is currently of the order of 50 nm in solution, but is higher in air, as described below.

Reaction Rate Imaging and Heterogeneous Kinetics

Since the tip response depends upon the rate of the electron-transfer reaction on the particular site being imaged on the substrate surface, by selecting the proper solution mediator, Ox/Red, and imaging conditions (e.g., the applied potential to the substrate) one can distinguish sites of different reactivity. The principles of this approach are illustrated in Figure 3. This was first demonstrated for a glassy carbon (GC) surface containing embedded Au sites, where Fe^{3+} was reduced at the tip, and the generated Fe^{2+} was oxidized on the GC/Au substrate [13]. Not only is it possible to show qualitative differences in the reaction rate at different locations on a surface, but by quantitative measurements of i_T as a function of d and substrate potential, one can obtain values for heterogeneous electron transfer rate constants of surface reactions. Recent theory [16] has been developed to extract kinetic parameters (m, k^o) relatively simply from steady-state cyclic voltammograms, and this approach can be used for microelectrode tips either in bulk solution or in a thin-layer SECM configuration utilizing either solid or liquid substrates.

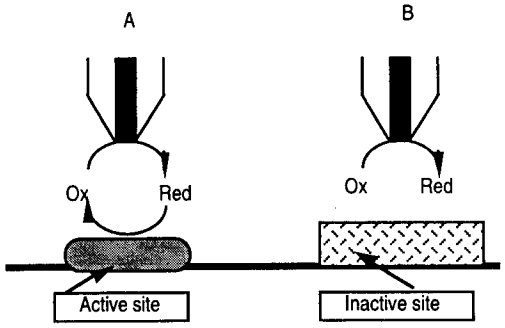

Fig. 3. Principle of reaction rate imaging. A. An active site produces positive feedback. B. An inactive site produces negative feedback.

Single Molecule Electrochemistry[17]

The electrochemical behavior of a single molecule can be observed by trapping a small volume of a dilute solution of the electroactive species in the SECM between an ultramicroelectrode tip with a diameter of ~15 nm and a conductive substrate. The principle of this experiment is illustrated in Fig. 4.

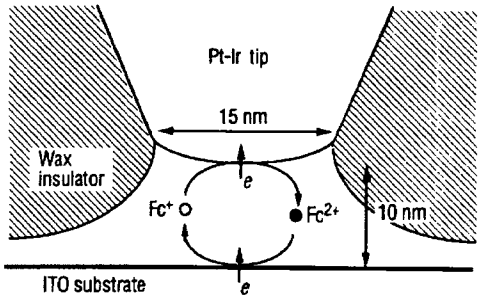

Fig. 4. Idealized schematic illustration of the tip geometry and tip-substrate configuration used in single-molecule detection with the SECM. [Reprinted from F.-R. F. Fan and A. J. Bard, *Science*, **267**, 871 (1995). Copyright 1995 American Association for the Advancement of Science.]

To achieve single-molecule detection (SMD) in the SECM, a small tip electrode with a geometry that provides confinement of the molecule near the active tip area is held near (~10 nm) a conductive substrate. The solution concentration is adjusted so that on the average only a single molecule will reside in the volume defined by the tip area and tip-substrate spacing d. Consider a tip of radius a of 5 nm held at d = 10 nm. For a 2 mM solution of an electroactive species, it is probable that only one molecule will be present in the ~10^{-18} cm^3 volume beneath the tip. The time required for the molecule to transit between tip and substrate is of the order of $d^2/2D$, where D is the diffusion coefficient of the molecule. Thus a molecule with $D = 5 \times 10^{-6}$ cm^2/s will transit the gap in about 100 ns or undergo ~10^7 round trips between tip and substrate per second. If an electron-transfer event occurs at each collision with the tip, a current of the order of 1 pA will flow. In this case, SMD depends upon the 10^7 amplification factor provided by the SECM positive feedback. The geometry of the electrode is important in this experiment. The electrode is constructed so that the conductive tip is slightly recessed in the insulating wax sheath, allowing the molecule to be physically confined between tip and substrate. The size of the tip and the geometry can be gained from ultramicroelectrode measurements (via eqn. 1) and from the SECM approach curve, which shows significant deviations at very small d values (see Figure 2 in [17]).

The results of carrying out such an experiment with a Pt tip, an indium tin oxide coated glass substrate, and a solution in which [(trimethylammonio)methyl] ferrocene (Cp_2FeTMA^+) is the electroactive molecule is shown in Figure 5. Fluctuations are observed when the electrode is moved close to the substrate, held at a potential where the oxidation of the Cp_2FeTMA^+ is diffusion-controlled (0.55 V versus SCE), and i_T is measured as a function of time (Fig. 5, curve A). Although the signal is noisy, the current shows clear peaks of 0.7 and 1.4 pA as well as periods of essentially zero average current. We believe these represent current responses when one or two Cp_2FeTMA^+ molecules are trapped in the 10 nm gap between the tip and substrate and drift into or out of the tip region. This is seen clearly when these data are subjected to autocorrelation or the power spectral density function. As a control experiment, curve B was taken when the tip was further from the substrate; it shows a constant average current over a 300 s measurement period. To show that the fluctuations seen at small d do not represent thermal drift of the tip (bringing it into and out of tunneling distance), we studied the behavior with the tip closer to the substrate in a solution containing only supporting electrolyte. In the absence of Cp_2FeTMA^+, the average current is essentially zero until tunneling distances are attained. At that point (curve C), the initial current is higher than that in curve A, with very large short term current spikes that probably

represent thermal fluctuations and vibrations. These are very different than the smoother broad peaks seen with electroactive species with the tip at slightly larger distances in curve A. Although single molecule voltammetry is still in its early stages, we have now carried out a number of experiments with different electroactive materials and substrates, and the results continue to support the proposed model.

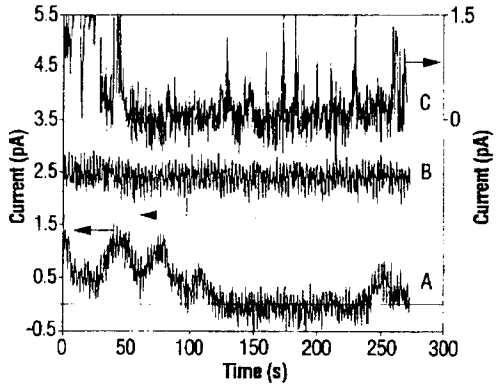

Fig. 5. Time evolution of the tip current observed at a tip potential of 0.55 V and a substrate potential of -0.3 V versus SCE. The initial tip current in A and C was set by approaching the substrate until $i_T \approx 1.5$ pA. Curve A: tip-substrate separation of ~10 nm in a solution containing 2 mM Cp_2FeTMA^+ and 2.0 M $NaNO_3$ (left current scale). Curve B: with the tip far from substrate in same solution as in A (left current scale). Curve C: tip-substrate separation within tunneling range in a solution containing only 2.0 M $NaNO_3$ (right current scale). The data sampling rate was 0.4 s per point. [Reprinted from F.-R. F. Fan and A. J. Bard, *Science*, **267**, 871 (1995). Copyright 1995 American Association for the Advancement of Science.]

SECM in Air

Although on first consideration the possibility of doing electrochemistry in a gaseous environment seems unlikely, SECM can also be performed on substrates in air, as long as very small currents, in the pA range, are employed. It is well-known that many substrates, e.g., mica, form a thin layer of water when exposed to humid air. For example, a recent report by Guckenberger and coworkers [18] described the use of an STM with high current sensitivity to image DNA on a mica surface in humid air. Although these authors identified the observed current with tunneling through the thin liquid layer on the surface, the required tunneling distance in the configuration of the cell used was much too large, and the experimental results are better described in terms of electrochemical reactions at tip and the other contact (which behaves as the counter electrode)[19]. The proposed mechanism for imaging in this case is shown in Figure 6. An advantage of this SECM imaging mode is that very high resolution can be attained using tips without insulation (i.e., the usual Pt-Ir or W STM-type tips) because the tip area is defined by the small part of the tip that touches the liquid layer. We have used this type of SECM to image DNA molecules and Nafion films on mica surfaces.

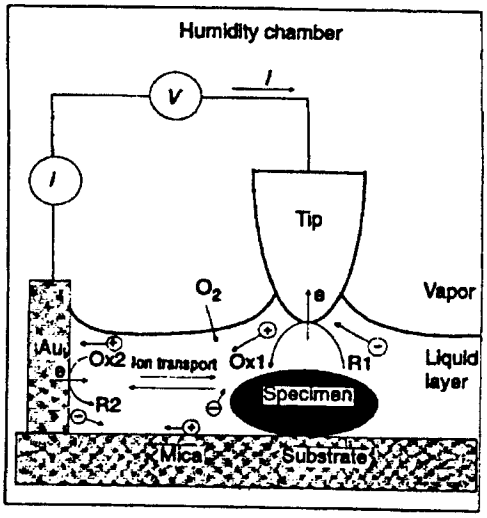

Fig. 6. Schematic diagram for the SECM chamber with controlled humidity and the electrochemical processes that control the current. The SECM tip was located ~1 to 2 mm from the Au contact. *V*: voltage bias between the tip and Au contact. *i*: current flow through the tip. R and Ox represent the reduced and oxidized forms of an electroactive species. $\oplus$ and $\ominus$ represent cations and anions in the water film. [Reprinted from F.-R. F. Fan and A. J. Bard, *Science*, in press. Copyright 1995 American Association for the Advancement of Science.]

Conclusions

This brief review outlines some of the applications of SECM to studies of surfaces and electrochemical systems. The field is expanding rapidly and studies of polymers, enzymes, membranes, and solid crystals have been reported. Similarly, the SECM can be used for nanofabrication, with the tip used to deposit or etch the substrate. In addition to the amperometric tips described in this paper, potentiometric (ion selective) tips and enzyme electrode tips have also been used.

Acknowledgment

I would like to thank my many coworkers, whose names are given in the following references, for their hard work and brilliant contributions to the development of SECM.

References

1. A. J. Bard, F.-R. F. Fan, J. Kwak and O. Lev, *Anal. Chem.*, **61**, 132 (1989).
2. A. J. Bard, F.-R. F. Fan, D. T. Pierce, P. R. Unwin, D. O. Wipf and F. Zhou, *Science*, **254**, 68 (1991).
3. A. J. Bard, G. Denuault, C. Lee, D. Mandler and D. O. Wipf, *Acc. Chem. Res.*, **23**, 357 (1990).
4. A. J. Bard, F.-R. F. Fan and M. V. Mirkin, in "Electroanalytical Chemistry", Vol. 18, A. J. Bard, Ed., Marcel Dekker, New York, 1994, p 243.
5. A. J. Bard and L. R. Faulkner, "Electrochemical Methods, Fundamentals and Applications", Wiley, New York, 1980.
6. R. M. Wightman and D. O. Wipf, in "Electroanalytical Chemistry", Vol. 15, A. J. Bard, Ed., Marcel Dekker, New York, 1988, p 267.
7. J. Kwak and A. J. Bard, *Anal. Chem.*, **61**, 1221 (1989).
8. M. V. Mirkin and A. J. Bard, *J. Electroanal. Chem.*, **323**, 1 (1992).
9. M. V. Mirkin and A. J. Bard, *J. Electroanal. Chem.*, **323**, 29 (1992).
10. A. J. Bard, M. V. Mirkin, P. R. Unwin and D. O. Wipf, *J. Phys. Chem.*, **96**, 1861 (1992).
11. A. J. Bard, G. Denuault, R. A. Friesner, B. C. Dornblaser and L. S. Tuckerman, *Anal. Chem.*, **63**, 1282 (1991).
12. P. R. Unwin and A. J. Bard, *J. Phys. Chem.*, **95**, 7814 (1991).
13. D. O. Wipf and A. J. Bard, *J. Electrochem. Soc.*, **138**, 469 (1991).
14. D. O. Wipf and A. J. Bard, *Anal. Chem.*, **64**, 1362 (1992).
15. D. O. Wipf and A. J. Bard, *Anal. Chem.*, **65**, 1373 (1993).
16. M. V. Mirkin and A. J. Bard, *Anal. Chem.*, **64**, 2293 (1992).
17. F.-R. F. Fan and A. J. Bard, *Science*, **267**, 871 (1995).
18. R. Guckenberger et al., *Science*, **266**, 1538 (1994) ; *J. Vac. Sci. Technol.* **B9**, 1227 (1991).
19. F.-R. F. Fan and A. J. Bard, *Science*, in press.